EUROPEAN ORGANIZATION FOR NUCLEAR RESEARCH

Proposal to the ISOLDE and Neutron Time-of-Flight Committee

Weak interaction studies via beta-delayed proton emission

September 23, 2020

P. Alfaurt[1], V. Araujo-Escalona[2], P. Ascher[1], D. Atanasov[3], B. Blank[1], F. Cresto[1], L. Daudin[1], X. Fléchard[4], A. Garcia[5], M. Gerbaux[1], J. Giovinazzo[1], S. Grévy[1], T. Kurtukian-Nieto[1], E. Liénard[4], D. Melconian[6], M. Pomorski[1], G. Quéméner[4], M. Roche[1], N. Severijns[2], S. Vanlangendonck[2], M. Versteegen[1], D. Zákoucký[7]

[1] *CENBG-IN2P3-CNRS, Université Bordeaux 1, Gradignan, France*
[2] *Instituut voor Kern- en Stralingsfysica, Katholieke Universiteit Leuven, Leuven, Belgium*
[3] *CERN, Geneva, Switzerland*
[4] *Normandie Univ, ENSICAEN, UNICAEN, CNRS/IN2P3, LPC Caen, Caen, France*
[5] *Department of Physics, University of Washington, Seattle, USA*
[6] *Cyclotron Institute, Texas A&M University, College Station, USA*
[7] *Nuclear Physics Institute, Acad. Sci. Czech Rep., Řež, Czech Republic*

Spokespersons: B. Blank (blank@cenbg.in2p3.fr), N. Severijns (nathal.severijns@kuleuven.be)
Contact person: D. Atanasov (dinko.atanasov@cern.ch)

CERN-INTC-2020-058 / INTC-P-574
24/09/2020

Abstract: We propose to perform simultaneous measurements of the β-ν angular correlation coefficient ($a_{\beta\nu}$) and the Fierz interference term (b) in ^{32}Ar pure Fermi and pure Gamow-Teller transitions using the *kinematic shift* technique. The proposal follows the successful proof-of-principle campaign, approved by the INTC committee as a LOI [1]. Results from that work allowed us to investigated statistical and systematic effects influencing the level of precision of the technique. We demonstrated its applicability by yielding the third most precise value of the $\tilde{a}^{\mathrm{F}}_{\beta\nu} = 1.007(32)_{stat}(25)_{sys}$ for the pure Fermi transition [2] with only 1.5 days of beam time. Considering the upgrades undertaken during LS2, such as a tailor-made detection setup and adequate ion-beam transport, our projection shows that the proposed measurements could reach a precision level of 10^{-3} for the pure Fermi transition. The measurements will therefore significantly improve previous experimental findings, $\sigma(\tilde{a}^{\mathrm{F}}_{\beta\nu}) = 0.65\%$, done with correlation measurements in nuclear beta decay and remain competitive with the search performed at the Large Hadron Collider (LHC).

Requested shifts: 24 shifts, (split into 1 run over 1 years)

1 Motivation

The search for new physics in the electroweak sector of the standard model (SM) continues in many forms despite its remarkable success [3]. Precision beta decay experiments are ideal tools to study the existence of new gauge bosons in a way that is complementary to high-energy, e.g. the LHC experiments. The minimal description of beta decay contains only vector (V) and axial-vector (A) currents. But, the full form of the beta-decay Hamiltonian allows other Lorentz invariant current contributions, such as scalar (S) and tensor (T). The present experimental limits on these coupling constants are derived from correlation measurements, that are known to the 0.65% level for pure Fermi and 0.91% for Gamow-teller transitions [4]. This level of precision does not allow one completely to rule out exotic currents, and furthermore still permits sizable contributions to be accommodated without affecting the phenomenological conclusions of the weak interaction.
The numerical value of the predicted beta-neutrino correlation coefficient ($a_{\beta\nu}$) for the strict V-A structure of the weak interaction, is fixed currently in the SM to $a_{\beta\nu} = 1$ for pure Fermi decays and $a_{\beta\nu} = -1/3$ for pure Gamow-Teller decays. The values of the Fierz interference term in both transitions are fixed to $b = 0$. Thus, any admixtures of S or T currents to the dominant V or A one, would result in a measurable deviation from the SM expectation value such that [1]

$$\begin{aligned} a^{F}_{\beta\nu} &\approx 1 - \frac{|C_S|^2 + |C'_S|^2}{|C_V|^2} & \qquad b^{F} &\approx \pm Re\left(\frac{C_S + C'_S}{C_V}\right) \\ a^{GT}_{\beta\nu} &\approx -\frac{1}{3}\left[1 - \frac{|C_T|^2 + |C'_T|^2}{|C_A|^2}\right] & \qquad b^{GT} &\approx \pm Re\left(\frac{C_T + C'_T}{C_A}\right) \end{aligned} \tag{1}$$

where C_i and C'_i, $(i = V, A, S, T)$ are the fundamental weak coupling constants. However, it is difficult to measure both $a_{\beta\nu}$ and b independently and the observable extracted from experiments is in fact $\tilde{a}_{\beta\nu}$ which is expressed as:

$$\tilde{a}_{\beta\nu} = \frac{a_{\beta\nu}}{(1 + \alpha b)} \tag{2}$$

where α denotes the weighted average over the measured part of the beta spectrum. The study of the $\tilde{a}_{\beta\nu}$ coefficient is possible only by the fact that the momentum of the neutrino can be inferred from measurements of the momentum of the recoiling daughter nucleus. It was shown, that if the daughter nucleus is unstable to particle emission (β-delayed), its momentum can be determined by the kinematics of the decay products [5]. When a light energetic particle is emitted from a moving source (i.e. the recoiling daughter nucleus) its energy will be subject to a *kinematic shift* that reflects the motion of the moving source. Thus, one can study the energy spectrum of subsequently emitted beta-delayed particles, instead of the slow heavy nuclei. One such example is the beta-delayed proton emitter ^{32}Ar, where in Fig.1 a schematic representation of the V- and S-type kinematics are shown. Applying the *kinematic shift* technique in the case of ^{32}Ar requires the detection of coincidences between: (i) the beta-delayed proton emitted by the recoiling

[1] Assuming maximal parity violation and no time-reversal symmetry violation of the standard V-A terms

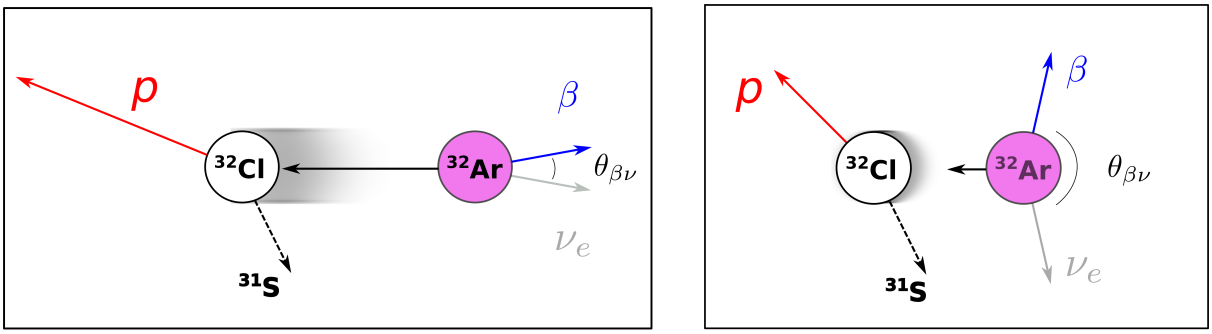

(a) Vector interaction

(b) Scalar interaction

Figure 1: Schematic representation of the decay kinematics of a pure Fermi transition and its influence on the beta-delayed proton energy. The maximum emission probability occurs at $\theta_{\beta\nu} = 0°$ corresponding to the dominant Vector interaction, while for Scalar it occurs close to $\theta_{\beta\nu} = 180°$.

^{32}Cl daughter nucleus and (ii) the preceding positron. The simultaneous measurement of $\tilde{a}_{\beta\nu}$ for the GT transitions in our experiment will be used as a systematic check of the validity of the analysis, see Section V in [2] for a detailed discussion.
Note that, an important advantage of the technique when compared to more traditional measurements, based on broadening effects [6], comes from the less crucial knowledge of the properties of the charged-particle detectors. Evidence of this fact can be seen in our proof-of-principle measurements, where despite the short beam time (≈35h of collected data) and the rudimentary setup, the achieved precision on $\tilde{a}^{\mathrm{F}}_{\beta\nu}$ of 4% is the third most precise value [2] (still in agreement with the SM). The observed kinematic shifts for the pure Fermi transition in the decay of ^{32}Ar from that experiment are presented in Fig.2. Even with the typical resolution of 35 keV, one clearly sees the effect from the recoil energy due to the dominant V current. Thus, the challenge is to resolve possible contributions due to S-type currents.

2 Experimental setup and upgrades during LS2

Using the results of the proof-of-principle experiment as a basis, our group identified necessary upgrades to be applied to the experimental setup during LS2, addressing the various sources contributing to the achieved statistical and systematic uncertainty on $\tilde{a}^{\mathrm{F}}_{\beta\nu}$. The most notable contributions are related to the ion-beam transport, the proton detectors and last but not least the positron backscattering.

The conceptual design from the proof-of-principle setup will be kept and can be seen in Fig.3. The ^{32}Ar sample will be continuously accumulated in the center of the superconducting magnet on a thin implantation foil (Catcher). The β-delayed protons will be detected by actively cooled single-sided silicon-strip detectors, placed on either side of the Catcher. The 4T magnetic field, applied along the axial direction of the detection setup, will guide the positrons through an opening to a thick plastic scintillator detector.

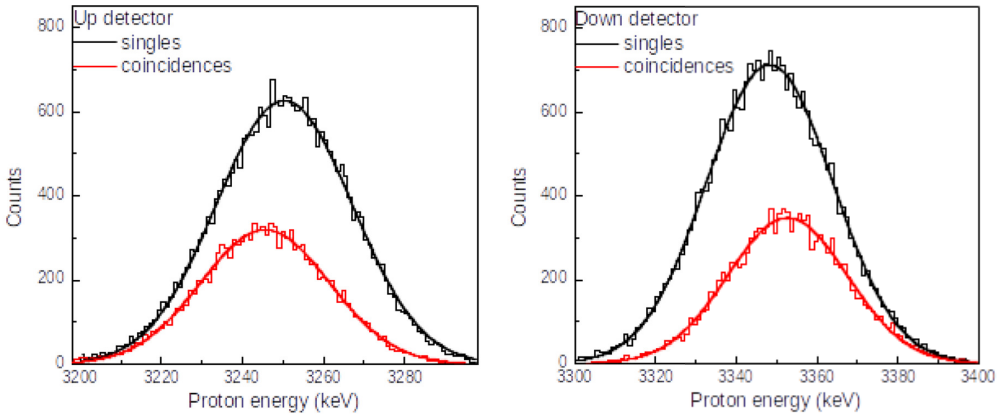

Figure 2: Proton energy of the superallowed transition for beta coincidences (red) and singles (black) obtained for one upper and one lower detector from the Proof-of-Principle experiment. The Gaussian fits are to guide the eye. The physics information is contained in the energy shift between the beta-proton coincidence peak compared to the singles peak.

The ^{32}Ar beam will be transported through roughly 12m of beamline to reach the implantation point. During the proof-of-principle experiment we have observed in the last section unusually high losses, reducing the total transmission to 12%. The group identified the possible reason and since then has taken actions to upgrade the responsible inadequate electrostatic elements. Using the new capabilities of the ion-beam optics, SIMION simulations predict that ion-beam transmission close to 100% could be reached in that section, allowing to a gain approximately a factor of 5.8.
The new detection system is currently under commissioning, but first estimations already show that a resolution of 10 keV (FWHM) for the proton detectors can be reached. Thus, due to the higher resolution one expects an improvement factor of 2.1 considering the same statistics as in the proof-of-principle experiment. Using the new geometry we expect to cover a solid angle close to 40%, which translates to gain factor of about 5 compared to the old detection system.
Another significant effect observed in the previous measurements came from the usage of a rather thick Catcher (6μm). In the new version, a commercial 500 nm thick Mylar foil will be used. Simulations show that using such thickness will reduce the systematic uncertainty by a factor 13, mainly due to reduction in the positrons backscattering in the foil. Furthermore, additional measurements with a 10μm foil will serve as a direct experimental estimate (without relying on simulations) on the level to which the foil thickness impacts the extraction of $\tilde{a}_{\beta\nu}$. In parallel, an ongoing experimental program aiming at the in-depth characterization of the positron detector will allow the reduction of the systematic contributions to $\tilde{a}_{\beta\nu}$ from energy threshold and backscattering on the detector to 0.7×10^{-3} and 0.9×10^{-3}, respectively.
Considering all improvement factors mentioned above, the measurement of $\tilde{a}_{\beta\nu}$ in the pure Fermi transition of ^{32}Ar could reach a level of precision of the order of 2×10^{-3}. In

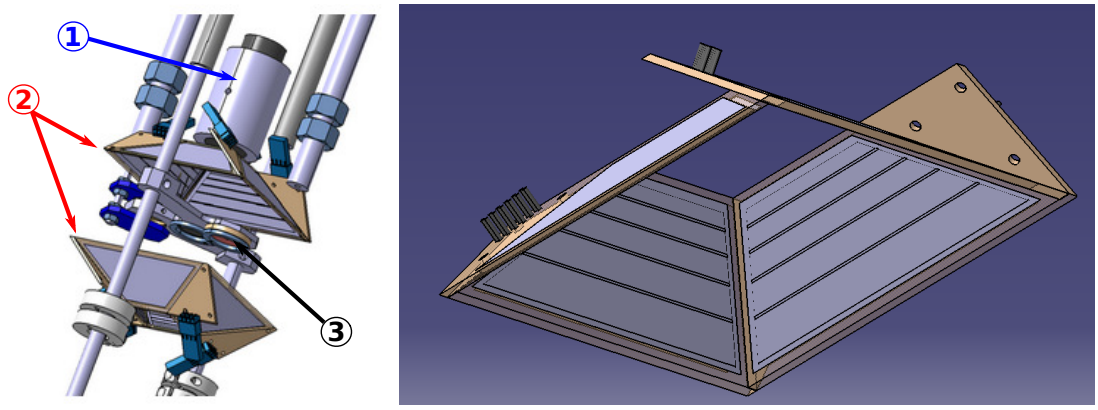

Figure 3: Computer Aided Design of the tailor-made detection setup. The left side shows the symmetrical configuration of the proton detectors (2) around the implantation point (3). The plastic scintillator (1) will be placed in the upper hemisphere. The right side is a zoom on one of the proton hemispheres, presenting its division in four sectors and each sector split in five segments. The trapezoidal shape and positioning was specifically designed to reduce systematic effects related to the proton incident angle.

Figure 4 the present constraints on scalar couplings are shown, comparing the result of the proof-of-principle experiment to previous experiments with ^{32}Ar and ^{38m}K. Furthermore, a visualisation of the exclusion plots is given, if one considers the targeted level of precision and compares it in addition to present and future search at the LHC [4]. With this level of precision and with a higher sensitivity to the Fierz interference term, the proposed measurement of $\tilde{a}^{\mathrm{F}}_{\beta\nu}$ will improve significantly the present constraints on exotic currents of the weak interaction inferred from correlation measurements and remain competitive with high-energy experiments.

3 Beam time request

We would like to request a beamtime to be scheduled in 2021, where the goal will be to reduce the statistical uncertainty of $\tilde{a}^{\mathrm{F}}_{\beta\nu}$ to an absolute uncertainty of 1×10^{-3}. To achieve this level of precision one would need a factor of 36 compared to the previous experiment in terms of statistical error. The new resolution of the proton detectors will lower the factor to a value of 17, which roughly translates to about 2.9E7 collected positron-proton events, i.e. 294 times more coincidence events with respect to the previous experiment. The new detector geometry will provide a factor 5. The improvements in the ion-beam transport will allow to gain a factor of 5.8. With a production of 2000 ions/μC of ^{32}Ar and an average primary beam intensity of 2μA we expect to gain a factor of 2.35. Finally, the duration of the beamtime, which will allow us to gather the minimum required statistics amounts to 6 days (18 shifts) or a factor of 4.1. To improve the uncertainties due to the calibration slope of the proton detectors, we would like to include 2 shifts on the neighbouring ^{33}Ar isotope to measure the well-known proton transitions. The ^{33}Ar shifts will be spread over the full requested beamtime, permitting the investigation of possible time drifts in the calibration. Finally, we would require 3 additional shifts for

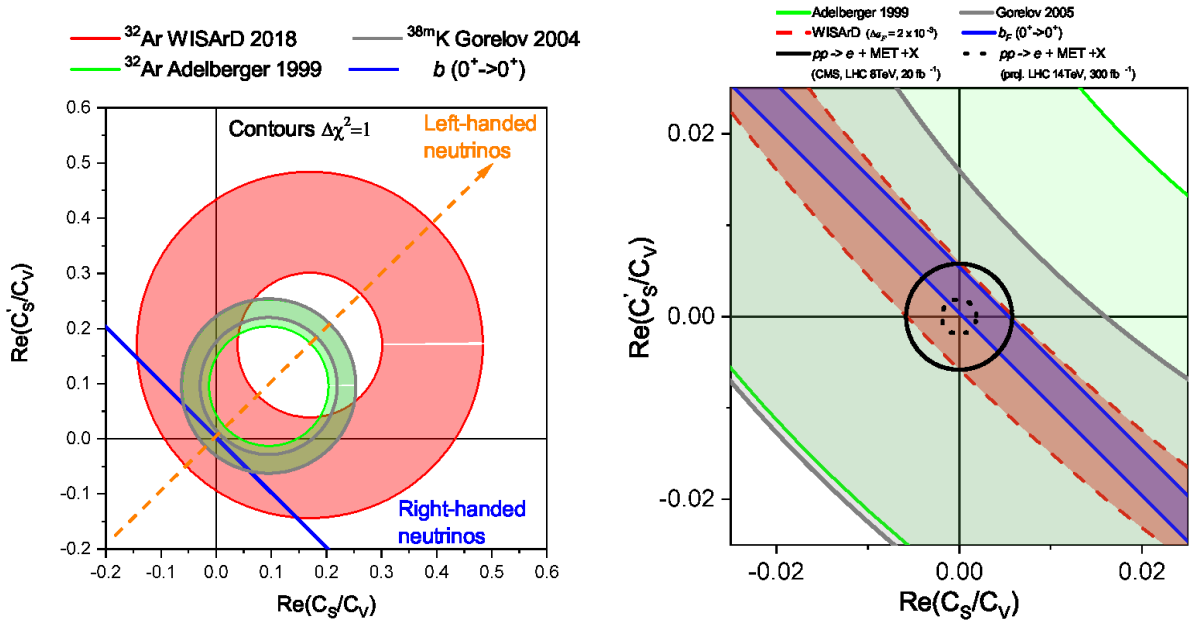

(a) Present constraints.

(b) Projected limits.

Figure 4: Exclusion plots for the scalar coupling constants. (a) Present picture from correlation measurements in nuclear beta decay (b) Projections of WISArD reaching a precision of 0.2%, showing that at this precision it will remain competitive to high-energy physics.

stable beam tuning, target and ion-source optimization.

Summary of requested shifts: 24 shifts in 1 run during 2021.

References

[1] B. Blank *et al.* CERN-INTC-2016-050 / INTC-I-172, (2016)

[2] V. Araujo-Escalona *et al.* Phys. Rev. C **101**, 055501 (2020)

[3] N. Severijns, M. Beck, O. Naviliat-Cuncic, *Rev. Mod. Phys* **78**, 3 (2006).

[4] M. González-Alonso, O. Naviliat-Cuncic, N. Severijns, *Prog. Part. Nucl. Phys* **104**, 165 (2019).

[5] E.T.H. Clifford *et al.* Nuc Phys **A493** (1989) 293-322

[6] E. G. Adelberger *et al. Phys. Rev. Lett.* **83**, 1299 (1999).

Appendix

DESCRIPTION OF THE PROPOSED EXPERIMENT

The experimental setup comprises: (*name the fixed-ISOLDE installations, as well as flexible elements of the experiment*)

Part of the	Availability	Design and manufacturing
(if relevant, name fixed ISOLDE installation: COLLAPS, CRIS, ISOLTRAP, MINIBALL + only CD, MINIBALL + T-REX, NICOLE, SSP-GLM chamber, SSP-GHM chamber, or WITCH)	☒ Existing	☒ To be used without any modification
[Part 1 of experiment/ equipment]	☐ Existing	☐ To be used without any modification ☐ To be modified
	☐ New	☐ Standard equipment supplied by a manufacturer ☐ CERN/collaboration responsible for the design and/or manufacturing
[Part 2 of experiment/ equipment]	☐ Existing	☐ To be used without any modification ☐ To be modified
	☐ New	☐ Standard equipment supplied by a manufacturer ☐ CERN/collaboration responsible for the design and/or manufacturing
[insert lines if needed]		

HAZARDS GENERATED BY THE EXPERIMENT (if using fixed installation:) Hazards named in the document relevant for the fixed [COLLAPS, CRIS, ISOLTRAP, MINIBALL + only CD, MINIBALL + T-REX, NICOLE, SSP-GLM chamber, SSP-GHM chamber, or WITCH] installation.

Additional hazards:

Hazards	[Part 1 of experiment/ equipment]	[Part 2 of experiment/ equipment]	[Part 3 of experiment/ equipment]
Thermodynamic and fluidic			
Pressure	[pressure][Bar], [volume][l]		
Vacuum			
Temperature	[temperature] [K]		
Heat transfer			
Thermal properties of materials			
Cryogenic fluid	[fluid], [pressure][Bar], [volume][l]		

Electrical and electromagnetic			
Electricity	[voltage] [V], [current][A]		
Static electricity			
Magnetic field	[magnetic field] [T]		
Batteries	☐		
Capacitors	☐		
Ionizing radiation			
Target material [material]			
Beam particle type (e, p, ions, etc)			
Beam intensity			
Beam energy			
Cooling liquids	[liquid]		
Gases	[gas]		
Calibration sources:	☐		
• Open source	☐		
• Sealed source	☐ [ISO standard]		
• Isotope			
• Activity			
Use of activated material:			
• Description	☐		
• Dose rate on contact and in 10 cm distance	[dose][mSV]		
• Isotope			
• Activity			
Non-ionizing radiation			
Laser			
UV light			
Microwaves (300MHz-30 GHz)			
Radiofrequency (1-300 MHz)			
Chemical			
Toxic	[chemical agent], [quantity]		
Harmful	[chem. agent], [quant.]		
CMR (carcinogens, mutagens and substances toxic to reproduction)	[chem. agent], [quant.]		
Corrosive	[chem. agent], [quant.]		
Irritant	[chem. agent], [quant.]		
Flammable	[chem. agent], [quant.]		

Oxidizing	[chem. agent], [quant.]		
Explosiveness	[chem. agent], [quant.]		
Asphyxiant	[chem. agent], [quant.]		
Dangerous for the environment	[chem. agent], [quant.]		
Mechanical			
Physical impact or mechanical energy (moving parts)	[location]		
Mechanical properties (Sharp, rough, slippery)	[location]		
Vibration	[location]		
Vehicles and Means of Transport	[location]		
Noise			
Frequency	[frequency],[Hz]		
Intensity			
Physical			
Confined spaces	[location]		
High workplaces	[location]		
Access to high workplaces	[location]		
Obstructions in passageways	[location]		
Manual handling	[location]		
Poor ergonomics	[location]		

Hazard identification:

Average electrical power requirements (excluding fixed ISOLDE-installation mentioned above): [make a rough estimate of the total power consumption of the additional equipment used in the experiment]